

## Inverse Design of Solidification Processes with Desired Freezing Front Motions and Heat Fluxes

**Nicholas Zabaras and George Z. Yang**

Sibley School of Mechanical and Aerospace Engineering  
188 Frank H. T. Rhodes Hall, Cornell University  
Ithaca, NY 14853-3801

### ABSTRACT

This paper presents a finite element solution to an inverse solidification design problem. In particular, we consider solidification with natural convection in a fixed mold of an initially superheated liquid material. The boundary heat flux  $q_o$  in the mold wall is designed such that a desired growth velocity and heat fluxes are achieved in the isothermal solidification front. From growth and stability analyses of solidification, it is well known that the above interface quantities define the type and scale of the obtained solidification microstructures. As such the control of interface quantities has a paramount importance in the eventual design of cast materials with desired mechanical properties.

The inverse problem is mathematically posed as the optimization problem of minimizing the square error between the calculated temperature at the interface and the given melting temperature. The gradient of this cost functional is calculated via the solution of an appropriate adjoint problem. The minimization is performed by the conjugate gradient method via the solution of the direct, adjoint and sensitivity problems.

In this paper, the inverse methodology is demonstrated with the following design solidification problem. Let us suppose that we know the solution of a direct Stefan problem (conduction based solidification). We will then calculate the required modifications to the boundary heat flux such that the growth velocity and interface heat fluxes in solidification in the presence of natural convection remain the same as those in the Stefan problem. In principle this design problem will demonstrate a technique that eliminates the effects of convection on the freezing interface morphology.

### INTRODUCTION

Inverse and design solidification problems are the subject of intense research. Here, we concentrate on design solidification problems where the objective is to control the cooling boundary conditions in order to achieve desired growth velocities and freezing interface heat fluxes ([1]–[4]). It is known from a microstructure development analysis that control of the freezing

interface fluxes and of the growth velocity can lead to desired cast structures and mechanical properties in the final cast product [5].

Most of the examined design solidification problems take the form of an inverse problem where one calculates the heat flux conditions in part of the boundary from over-specified boundary conditions at another part of the boundary. Inverse convection problems were addressed earlier by Cuvelier [6] and more recently by Gunzburger and colleagues [7]–[8]. In the definition of their problem, the flow field was assumed known and it was not dynamically coupled with the heat transfer analysis.

The main features of the present work is the dynamic coupling of the fluid flow and heat transfer analysis in the inverse and direct analyses. The design problem is stated as a functional optimization problem in the  $L_2$  space. The gradient of the cost functional is obtained via the solution of an adjoint continuous problem. Temperature and fluid velocity sensitivity fields are also defined and used in the implementation of the conjugate gradient method.

A streamline upwind/Petrov-Galerkin finite element method is used to solve the direct, sensitivity and adjoint problems. An example problem is finally presented to demonstrate the potential applications of the present methodology.

### INVERSE FORMULATION

Let us consider that the domain  $\Omega$  is occupied by the liquid melt of a pure substance and that solidification starts at time  $t = 0$ . Let us denote the temperature and velocity fields as  $T(\mathbf{x}, t)$ , and  $\mathbf{v}(\mathbf{x}, t)$ , respectively. Let  $\Gamma$  be the boundary of  $\Omega$ . Based on the type of the applied thermal boundary conditions,  $\Gamma$  is divided into the solid-liquid freezing interface  $\Gamma_I$  that is at the melting temperature  $T_m$ , the boundary  $\Gamma_g$  where essential boundary conditions are applied, the boundary  $\Gamma_h$  of natural (flux) boundary conditions, and the boundary  $\Gamma_o$  where an *unknown* flux  $q_o$  is applied.

Let us introduce a length scale  $l$  and a time scale  $l^2/\alpha$  where  $\alpha$  is the thermal diffusivity of the liquid melt.

The dimensionless temperature is defined as  $\theta = \frac{T-T_m}{T_i-T_m}$  ( $T_i$  is a reference temperature), and the dimensionless velocity by  $\mathbf{u} = \frac{\mathbf{v}_l}{\alpha}$ . The dimensionless governing equations are:

$$\frac{\partial \theta}{\partial t} + \mathbf{u} \cdot \nabla \theta = \nabla \cdot \nabla \theta \quad (1)$$

$$\frac{\partial \mathbf{u}}{\partial t} + \mathbf{u} \cdot \nabla \mathbf{u} = \nabla \cdot \boldsymbol{\sigma} - RaPr\theta \mathbf{e}_g \quad (2)$$

$$\boldsymbol{\sigma} = -p\mathbf{I} + Pr[\nabla \mathbf{u} + (\nabla \mathbf{u})^T] \quad (3)$$

$$\nabla \cdot \mathbf{u} = 0 \quad (4)$$

$$\theta(\mathbf{x}, 0) = \theta_{in}(\mathbf{x}), \mathbf{x} \in \Omega \quad (5)$$

$$\mathbf{u}(\mathbf{x}, 0) = 0, \mathbf{x} \in \Omega \quad (6)$$

$$\mathbf{u}(\mathbf{x}, t) = 0, (\mathbf{x}, t) \in \Gamma \times [0, t_{max}] \quad (7)$$

$$\theta(\mathbf{x}, t) = \theta_g, (\mathbf{x}, t) \in \Gamma_g \times [0, t_{max}] \quad (8)$$

$$\frac{\partial \theta}{\partial n}(\mathbf{x}, t) = q_h(\mathbf{x}, t), (\mathbf{x}, t) \in \Gamma_h \times [0, t_{max}] \quad (9)$$

$$\frac{\partial \theta}{\partial n}(\mathbf{x}, t) = q_I(\mathbf{x}, t), (\mathbf{x}, t) \in \Gamma_I \times [0, t_{max}] \quad (10)$$

$$\frac{\partial \theta}{\partial n}(\mathbf{x}, t) = q_o(\mathbf{x}, t), (\mathbf{x}, t) \in \Gamma_o \times [0, t_{max}] \quad (11)$$

Here,  $Pr$  is the Prantdl number (ratio of kinematic viscosity  $\nu$  and  $\alpha$ ),  $Ra = \frac{g\beta(T_i-T_m)l^3}{\alpha\nu}$  is the Rayleigh number with  $\beta$  the thermal expansion coefficient,  $\boldsymbol{\sigma}$  is the dimensionless stress tensor,  $p$  is the dimensionless pressure,  $\mathbf{I}$  is the unit tensor and  $\mathbf{e}_g$  is the unit vector in the direction of gravity. Here  $\theta(\mathbf{x}, t; q_o)$  and  $\mathbf{u}(\mathbf{x}, t; q_o)$  are solutions of the direct problem for each boundary heat flux condition  $q_o$  at  $\Gamma_o$ .

In the *design problem* of interest, the temporal position of  $\Gamma_I$  is known. The main goal is to calculate the heat flux  $q_o$  that is imposed on  $\Gamma_o$ . This can be done by minimizing  $S(q_o)$  which measures the discrepancy between the calculated temperature  $T(\mathbf{x}, t; q_o)$ ,  $(\mathbf{x}, t) \in \Gamma_I \times [0, t_{max}]$  and the given interface temperature  $\theta = 0$  ( $T = T_m$ ):

$$\begin{aligned} S(q_o) &= \frac{1}{2} \|\theta(\mathbf{x}, t)\|_{L_2(\Gamma_I \times [0, t_{max}])}^2 \\ &= \frac{1}{2} \int_0^{t_{max}} \int_{\Gamma_I} \theta(\mathbf{x}, t)^2 d\Gamma dt \end{aligned} \quad (12)$$

It can be shown [9] that the derivative  $S'(q_o)$  of the cost functional in the  $L_2(\Gamma_I \times [0, t_{max}])$  space is:

$$S'(q_o(\mathbf{x}, t)) = \Psi(\mathbf{x}, t), \quad (\mathbf{x}, t) \in \Gamma_o \times (0, t_{max}) \quad (13)$$

The  $\Psi(\mathbf{x}, t)$  is the *adjoint temperature*, which is coupled with an adjoint velocity field  $\phi(\mathbf{x}, t)$ . They are calculated from the following well-posed *adjoint problem* [9]

$$\frac{\partial \Psi}{\partial t} + \mathbf{u} \cdot \nabla \Psi = -\nabla^2 \Psi + \phi \cdot \mathbf{e}_g \quad (14)$$

$$\frac{\partial \phi}{\partial t} + \mathbf{u} \cdot \nabla \phi - (\nabla \mathbf{u})^T \phi = -\nabla \cdot \zeta + PrRa\Psi\nabla\theta \quad (15)$$

$$\zeta(\mathbf{x}, t) = -\pi\mathbf{I} + Pr[\nabla\phi + (\nabla\phi)^T] \quad (16)$$

$$\nabla \cdot \phi = 0 \quad (17)$$

$$\Psi(\mathbf{x}, t_{max}) = 0, \quad \mathbf{x} \in \Omega \quad (18)$$

$$\phi(\mathbf{x}, t_{max}) = 0, \quad \mathbf{x} \in \Omega \quad (19)$$

$$\phi(\mathbf{x}, t) = 0, \quad (\mathbf{x}, t) \in \Gamma \times [0, t_{max}] \quad (20)$$

$$\Psi(\mathbf{x}, t) = 0, \quad (\mathbf{x}, t) \in \Gamma_g \times [0, t_{max}] \quad (21)$$

$$\frac{\partial \Psi}{\partial n}(\mathbf{x}, t) = 0, \quad (\mathbf{x}, t) \in (\Gamma_h + \Gamma_o) \times [0, t_{max}] \quad (22)$$

$$\frac{\partial \Psi}{\partial n} - (\mathbf{v}_f \cdot \mathbf{n})\Psi = \theta, \quad (\mathbf{x}, t) \in \Gamma_I \times [0, t_{max}] \quad (23)$$

where  $\zeta$  is the adjoint stress tensor,  $\pi$  is the adjoint pressure,  $\mathbf{n}$  is the normal pointing out of  $\Gamma_I$  and  $\mathbf{v}_f$  is the dimensionless known velocity of  $\Gamma_I$ .

To perform the optimization procedure and minimize  $S(q_o)$ , we will also need to define a *sensitivity problem*. The sensitivity temperature field  $\Theta(\mathbf{x}, t; q_o, \Delta q_o) \equiv D_{\Delta q_o} \theta(\mathbf{x}, t; q_o)$ , and the sensitivity velocity field  $\mathbf{U}(\mathbf{x}, t; q_o, \Delta q_o) \equiv D_{\Delta q_o} \mathbf{u}(\mathbf{x}, t; q_o)$  are defined as the linear in  $\Delta q_o$  parts of  $\theta(\mathbf{x}, t; q_o + \Delta q_o)$  and  $\mathbf{u}(\mathbf{x}, t; q_o + \Delta q_o)$  calculated at  $q_o$ , i.e.

$$\begin{aligned} \theta(\mathbf{x}, t; q_o + \Delta q_o) &= \theta(\mathbf{x}, t; q_o) + \Theta(\mathbf{x}, t; q_o, \Delta q_o) \\ &\quad + O(\|\Delta q_o\|_{L_2(\Gamma_o \times [0, t_{max}])}^2) \end{aligned} \quad (24)$$

$$\begin{aligned} \mathbf{u}(\mathbf{x}, t; q_o + \Delta q_o) &= \mathbf{u}(\mathbf{x}, t; q_o) + \mathbf{U}(\mathbf{x}, t; q_o, \Delta q_o) \\ &\quad + O(\|\Delta q_o\|_{L_2(\Gamma_o \times [0, t_{max}])}^2) \end{aligned} \quad (25)$$

The governing equations for the *sensitivity problem* are as follows:

$$\frac{\partial \Theta}{\partial t} + \mathbf{u} \cdot \nabla \Theta + \mathbf{U} \cdot \nabla \theta = \nabla \cdot \nabla \Theta \quad (26)$$

$$\begin{aligned} \frac{\partial \mathbf{U}}{\partial t} + \mathbf{u} \cdot \nabla \mathbf{U} + \mathbf{U} \cdot \nabla \mathbf{u} &= \nabla \cdot \boldsymbol{\Sigma} - PrRa\Theta\mathbf{e}_g \\ \boldsymbol{\Sigma} &= -\Pi\mathbf{I} + Pr[\nabla \mathbf{U} + (\nabla \mathbf{U})^T] \end{aligned} \quad (27)$$

$$\nabla \cdot \mathbf{U} = 0 \quad (28)$$

$$\nabla \cdot \mathbf{U} = 0 \quad (29)$$

$$\Theta(\mathbf{x}, 0) = 0, \quad \mathbf{x} \in \Omega \quad (30)$$

$$\mathbf{U}(\mathbf{x}, 0) = 0, \quad \mathbf{x} \in \Omega \quad (31)$$

$$\mathbf{U}(\mathbf{x}, t) = 0, \quad (\mathbf{x}, t) \in \Gamma \times [0, t_{max}] \quad (32)$$

$$\Theta(\mathbf{x}, t) = 0, \quad (\mathbf{x}, t) \in \Gamma_g \times [0, t_{max}] \quad (33)$$

$$\frac{\partial \Theta}{\partial n}(\mathbf{x}, t) = 0, \quad (\mathbf{x}, t) \in (\Gamma_h + \Gamma_I) \times [0, t_{max}] \quad (34)$$

$$\frac{\partial \Theta}{\partial n}(\mathbf{x}, t) = \Delta q_o(\mathbf{x}, t), \quad (\mathbf{x}, t) \in \Gamma_o \times [0, t_{max}] \quad (35)$$

where  $\Sigma$  is the sensitivity stress tensor and  $\Pi$  is the sensitivity pressure.

We have outlined the definition of the continuous *direct*, *adjoint* and *sensitivity problems*. The conjugate gradient method (CGM) is used for the minimization of the cost functional  $S(q_o)$ . It constructs a sequence:  $q_o^0, q_o^1, \dots, q_o^k, \dots$ , to approach the optimal minimizer  $q_o$  [10]. The procedure is the following:

Step A: Make an initial guess of  $q_o^0(\mathbf{x}, t) \in L_2(\Gamma_o \times [0, t_{max}])$  and set  $k = 0$

Step B: Calculate the conjugate search direction  $p^k(\mathbf{x}, t), (\mathbf{x}, t) \in \Gamma_o \times [0, t_{max}]$

1. Solve the direct problem for  $\theta(\mathbf{x}, t; q_o^k)$  and  $\mathbf{u}(\mathbf{x}, t; q_o^k)$
2. Compute the residual  $\theta(\mathbf{x}, t; q_o^k)$  for  $(\mathbf{x}, t) \in \Gamma_I \times [0, t_{max}]$
3. Solve the adjoint problem backwards in time for  $\Psi(\mathbf{x}, t; q_o^k)$
4. Set  $S'(q_o^k) = \Psi(\mathbf{x}, t; q_o^k)$
5. Set  $\gamma^k = 0$ , if  $k = 0$ ; otherwise:

$$\gamma^k = \frac{(S'(q_o^k), S'(q_o^k) - S'(q_o^{k-1}))_{L_2(\Gamma_o \times [0, t_{max}])}}{\|S'(q_o^{k-1})\|_{L_2(\Gamma_o \times [0, t_{max}])}^2}$$

6. Define  $p^k(\mathbf{x}, t)$ , If  $k = 0$ ,  $p^0 = -S'(q_o^k)$ ; Otherwise,  $p^k = -S'(q_o^k)(\mathbf{x}, t) + \gamma^k p^{k-1}$

Step C: Calculate the optimal step size  $\alpha^k$

1. Solve the sensitivity problem for  $\Theta(\mathbf{x}, t; q_o^k, p^k)$  and  $\mathbf{U}(\mathbf{x}, t; q_o^k, p^k)$
2. Calculate  $\alpha^k$  by

$$\alpha^k = \frac{-(S'(q_o^k), p^k)_{L_2(\Gamma_o \times [0, t_{max}])}}{\|\Theta(\mathbf{x}, t; q_o^k, p^k)\|_{L_2(\Gamma_I \times [0, t_{max}])}^2}$$

Step D: Update  $q_o^{k+1}(\mathbf{x}, t) = q_o^k(\mathbf{x}, t) + \alpha^k p^k(\mathbf{x}, t)$ ,  $(\mathbf{x}, t) \in \Gamma_o \times [0, t_{max}]$

Step E: If  $\|q_o^{k+1} - q_o^k\|_{L_2(\Gamma_o \times [0, t_{max}])} < \epsilon$  (specified tolerance), stop; Otherwise, set  $k = k + 1$  and go to Step B.

The inner product in the  $L_2$  space involved in the CGM procedure is defined as:

$$(f, g)_{L_2(\Gamma \times [0, t_{max}])} = \int_0^{t_{max}} \int_{\Gamma} f g d\Gamma dt \quad (36)$$

## NUMERICAL IMPLEMENTATION

Let us consider liquid aluminum at a uniform initial temperature  $T_i (T_i > T_m)$ , that is confined in a

rectangular mold. The top and bottom walls are always kept adiabatic. The schematic configuration is shown in Figure 1. From  $t = 0^+$ , the left vertical wall ( $x = 0$ ) is dropped to a temperature  $T_0 (T_0 < T_m)$ , and maintained at that temperature for  $t > 0$ . We have taken the thermo-physical properties as: conductivity  $k_s = k_l = 0.0548 \text{ kcal/ms}^\circ\text{C}$ , specific heat  $c_s = c_l = 0.2526 \text{ kcal/kg}^\circ\text{C}$ , density  $\rho = 2650 \text{ kg/m}^3$ , latent heat  $L = 95.0 \text{ kcal/kg}$ , thermal expansion coefficient  $\beta = 3.84 \times 10^{-5} \text{ }^\circ\text{C}^{-1}$ ,  $Pr = 0.0149$ ,  $T_m = 660^\circ\text{C}$ . Also,  $T_i = 697.5^\circ\text{C}$ ,  $T_0 = 472.5^\circ\text{C}$ . The dimensions of the enclosure are chosen as  $5 \text{ cm} \times 10 \text{ cm}$ . The length scale is chosen as  $l = 5 \text{ cm}$ . The above properties correspond to an inverse Stefan number in the liquid of  $\epsilon = c_l(T_i - T_m)/L = 0.1$ , a constant dimensionless solid boundary cooling temperature  $\theta_0 = (T_0 - T_m)/(T_i - T_m) = -5.0$ , and  $Ra = 10^4$ .

If there is no convection in the liquid region ( $Ra = 0$ ) and the right vertical wall  $x = 1$  is kept adiabatic, the direct problem is reduced to a one-dimensional two phase Stefan problem. A singular perturbation solution [11] is available which describes the solid-liquid interface  $s(t)$  as follows:

$$s(t) = \epsilon^{\frac{1}{2}}(-2\theta_0 t)^{\frac{1}{2}} + \epsilon \sum_{j=0}^{\infty} \left\{ \frac{2}{(j + \frac{1}{2})\pi} e^{-[(j + \frac{1}{2})\pi]^2 t} - \frac{\sqrt{\pi/t}}{[(j + \frac{1}{2})\pi]^3} \text{erf}[(j + \frac{1}{2})\pi\sqrt{t}] \right\} + O(\epsilon^{\frac{3}{2}}) \quad (37)$$

With this position (Figure 2), one can perform a direct moving/deforming FEM heat conduction analysis. The left boundary of the liquid region is moving with  $v_f = \dot{s}(t)$  and a fixed dimensionless melting temperature  $\theta_m = 0$ , while on the right boundary  $x = 1$ , the heat flux is given as  $q_o = 0$ . From the above direct analysis with the initial mesh shown in Figure 3, a uniform heat flux  $q_I(t)$  along the moving interface  $x = s^+$  can be obtained (Figure 4).

In the presence of natural convection ( $Ra \neq 0$ ), the flat solid-liquid interface will be distorted and  $q_I(y, t)$  will not be uniform along the interface.

As such we pose the following question: Can we adjust the boundary cooling conditions  $q_o = 0$  such that, in the presence of convection, solidification results in a flat interface moving as described by equ. (37) and with the uniform heat flux  $q_I(t)$  as given in Figure 4?

Here, we assume that there is a non-zero  $q_o(y, t)$  that will compensate for the convection induced geometrical and thermal deviation of the solid-liquid interface from the state corresponding to the pure conduction case. In the remaining of the section, only the inverse design problem in the liquid region needs to be solved. Similar inverse problems in the solid phase have been addressed elsewhere [4].

A fixed constant number of  $20 \times 20$  non-uniform

quadrilateral elements is used, as shown in Figure 3 for  $t = 0$ . Bilinear shape functions are used for both temperature and velocity. The penalty number for the incompressibility condition is  $10^8$ . A moving finite element approach is taken to handle the shrinking of the liquid region. A streamlined upwind Petrov-Galerkin scheme is used for the direct, adjoint and sensitivity problems [12]. The details of the matrix formulation and time integration for the direct, adjoint and sensitivity problems can be found in [9]. The time steps are  $\Delta t = 2 \times 10^{-4}$  up to  $t = 0.01$  and  $\Delta t = 0.001$  afterwards. A total of 800 steps was used until  $t_{max} = 0.76$  when solidification proceeds up to  $s(t_{max}) \simeq 0.85$ . The inverse calculation is computationally intensive, each global iteration with solutions of direct, adjoint and sensitivity problems requiring about 102.4 minutes CPU time on a DEC alpha 200 workstation with double precision arithmetic.

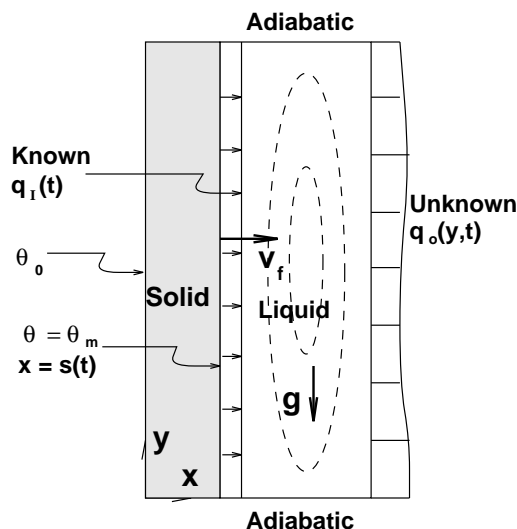


FIGURE 1: Schematic of the Example Problem.

## RESULTS AND DISCUSSION

The CGM iterations start with an initial guess  $q_o(y, t) = 0$  and go up to 150 iterations when  $\|q_o^{k+1} - q_o^k\| < 10^{-4}$ . The optimal temporal and spatial variations of the heat flux  $q_o(y, t)$  at the right vertical wall  $x = 1$  are shown in Figure 5. Figure 6 shows  $q_o(y, t)$ 's spatial variation at different fixed time levels. Figure 7 presents the objective function's values versus the iteration steps of the conjugate gradient method.

The temperature and flow fields in the liquid corresponding to this optimal heat flux are displayed in Figure 8 for different time levels. Each (a) of Figure 8 draws 15 levels of isotherms in the liquid region that are equally spaced in terms of temperature value. The lowest level  $\theta = 0$  is at the solid-liquid interface  $x = s(t)$  and the highest level touches  $x = 1$  with its value indicated as  $\theta_{max}$  on top of each figure.

Part (b) of Figure 8 displays the contours of the stream function  $\psi$ . For each (b), there are 10 levels of contours with equal spaced  $\psi$  values. The  $\psi_{max} = 0$  contour is just the boundary of the liquid melt:  $x = s(t), 1$  and  $y = 0, 1$ . As we can see, there is only one major convection melt flow cell (anti-clockwise). The flow field doesn't have a top-bottom symmetry. The magnitude of the x-component velocity  $|\frac{\partial \psi}{\partial y}|$  is larger at the lower rather than the upper parts of the cavity. This creates different strength of thermal advection between the upper and lower positions of the cavity. It also explains why the initially vertical isotherms will get distorted. In Figure 8 (a)'s, isotherms are touching the right vertical wall: it is heated stronger at the lower corner than the middle part, while the upper corner generally gets cooled as shown in Figure 6. This boundary heating or cooling distribution in the y-direction, adjusts the shapes of the isotherms by conduction and balances the convection effects. Note that the vertical isotherm  $\theta = 0$  at the solid-liquid interface  $x = s(t)$  was part of the design solution as becomes obvious by the definition of the cost functional  $S(q_o)$ .

The temporal characteristics show a strong growth of convective flow first, a maximum of flow at about  $t = 0.15 \sim 0.25$  before the flow eventually starts to die out.

Similar trends exist for the thermal input  $q_o(y, t)$  at the boundary  $x = 1$ . However, as can be seen from Figures 5 and 6, the corner boundary heating and cooling are maximum at the very beginning of the solidification process. This is due to the whole time domain minimization process and can be easily understood. The boundary heat flux  $q_o$  is adjusted early in time so that at later times it can influence the convection effects on the freezing interface.<sup>1</sup>

The solution  $q_o(y, t)$  is close to zero when  $t > 0.45$  because the temperature field is already nearly uniform and convection is very weak. This rules out the possibility that our solution is suffering from the end time condition induced by the initial guess of  $q_o(y, t_{max}) = 0$  [9], i.e.  $t_{max} = 0.76$  is large enough to overcome the end condition difficulty characteristics of adjoint formulations.

## CONCLUSIONS

In this work an infinite dimensional formulation is presented for the design of solidification processes with desired freezing front heat fluxes and growth velocity. Consistent direct, sensitivity and adjoint differential (continuum) natural convection problems were defined and solved using a streamline-upwind/ Petrov-Galerkin FEM algorithm. It is the first time that such formulations have been possible for convection based solidifi-

<sup>1</sup>There is a certain amount of time before heat flux changes in  $y$  and time can be felt in the calculated temperature  $T(\mathbf{x}, t; q_o)$  at the freezing interface. The required time is higher at earlier times when the interface is at a considerable distance from the fixed wall ( $x = 1$ ).

cation design and the success of the preliminary results points to a number of significant applications in casting process design. In addition to a further rigorous testing of the proposed algorithms, we plan to extend the presented methodology to alloy solidification and examine design problems related with the freezing interface stability and growth (control of the cast microstructures) and with macrosegregation and porosity development in castings.

#### ACKNOWLEDGMENTS

The results presented in this paper were obtained in the course of research sponsored by the National Science Foundation under grants CTS-9115438 and DMI-9157189 to Cornell University, with additional support from Alcoa Laboratories and the Cornell College of Engineering. The computing for this project was supported by the Cornell Theory Center. The authors gratefully acknowledge these contributions.

#### REFERENCES

1. N. Zabarar, Y. Ruan and O. Richmond, On the design of two-dimensional Stefan processes with desired freezing front motions, *Numerical Heat Transfer*, 21B (1992) 307-325.
2. N. Zabarar and S. Kang, On the solution of an ill-posed inverse design solidification problem using minimization techniques in finite and infinite dimensional spaces, *Int. J. Numer. Methods. Engr.*, 36 (1994) 3973-3990.
3. S. Kang and N. Zabarar, Control of the freezing interface motion in two-dimensional solidification processes using the adjoint method, *Int. J. Numer. Methods. Engr.*, 38 (1995) 63-80.
4. N. Zabarar and T. Hung Nguyen, Control of the freezing interface morphology in solidification processes in the presence of natural convection, *Int. J. Numer. Methods. Engr.*, 38 (1995) 1555-1578.
5. W. Kurz and D. J. Fisher, *Fundamentals of Solidification*, (Trans Tech Publications Ltd, Switzerland, 1989).
6. P. Cuvelier, Optimal control of a system governed by the Navier-Stokes equations coupled with the heat equations, in: W. Eckhaus (Ed.), *New Developments in Differential Equations* (North-Holland, Amsterdam, 1976) 81-98.
7. M. D. Gunzburger, L. Hou and T. Svobodny, Heating and cooling control of temperature distributions along boundaries of flow domains, *J. Math. Syst. Estim. Control*, 3(2) (1993) 147-172.
8. M. D. Gunzburger and H. C. Lee, Analysis, approximation, and computation of a coupled solid/fluid temperature control problem, *Comp. Methods Appl. Mech. Engr.*, 118 (1994) 133-152.
9. N. Zabarar and G. Yang, A functional optimization and implementation for an inverse natural convection problem, submitted to *Comp. Methods Appl. Mech. Engr.*
10. R. Fletcher, *Practical Methods of Optimization*, (Wiley-Interscience, New York, 1987).
11. S. Weinbaum, and L. M. Jiji, 1977, Singular perturbation theory for melting or freezing in finite domains initially not at fusion temperature, *ASME Journal of Applied Mechanics*, Vol. 44, 25-30.
12. C. Johnson, *Numerical Solution of Partial Differential Equations by the Finite Element Method* (Studentlitteratur, Sweden, 1987).

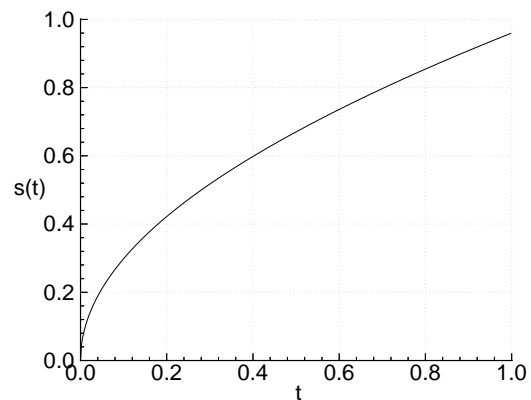


FIGURE 2: Interface position  $s(t)$

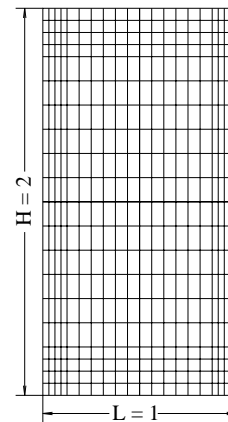


FIGURE 3: Non-uniform finite element mesh at  $t = 0$

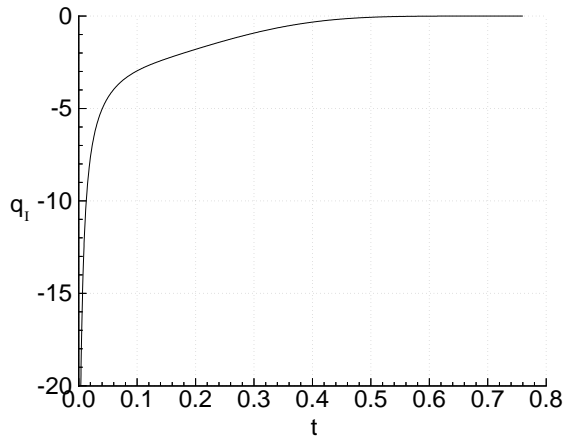


FIGURE 4: Interfacial heat flux (liquid side)  $q_I(t)$

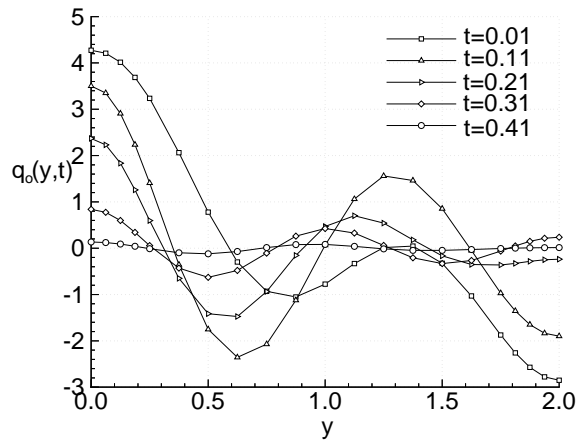


FIGURE 6:  $q_o(y, t)$  distribution at different time level

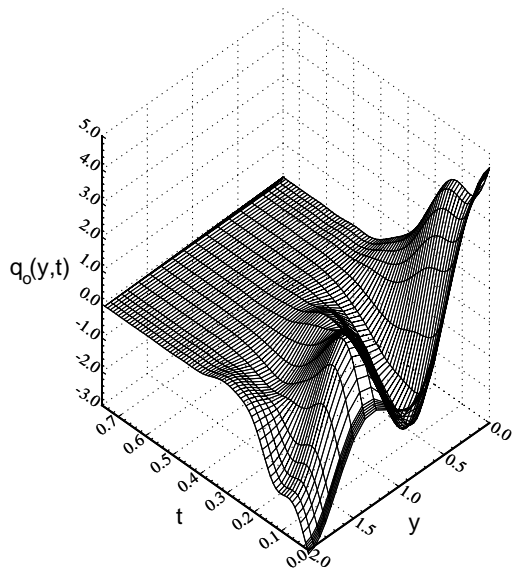


FIGURE 5: Optimal heat flux  $q_o(y, t)$  at vertical mold wall

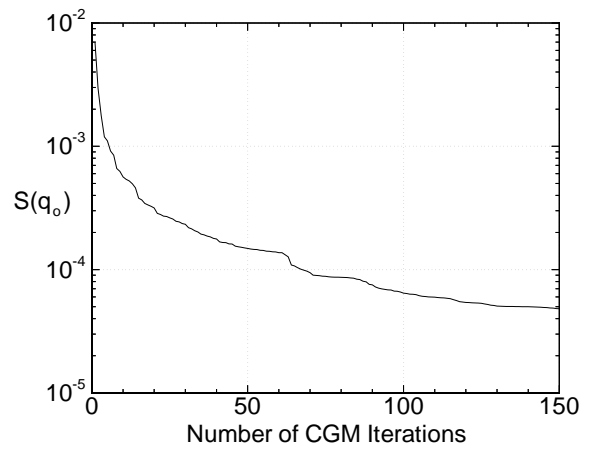
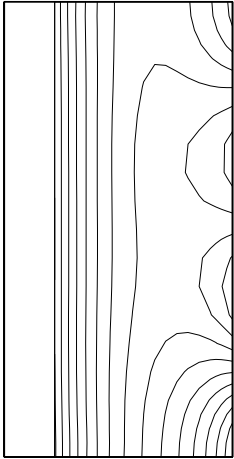


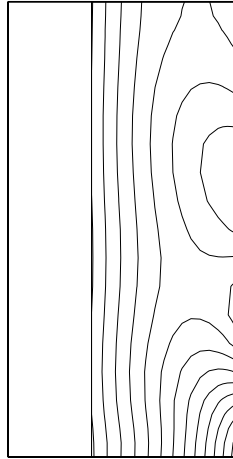
FIGURE 7: Objective function's Minimization with CGM Iterations

$t=0.05, s=0.221, \theta_{\max}=1.749$



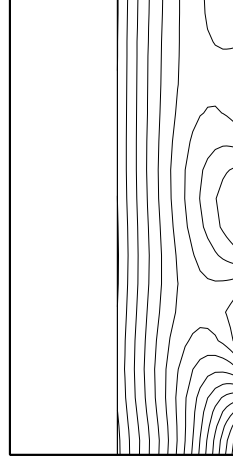
(1a)

$t=0.15, s=0.365, \theta_{\max}=1.474$



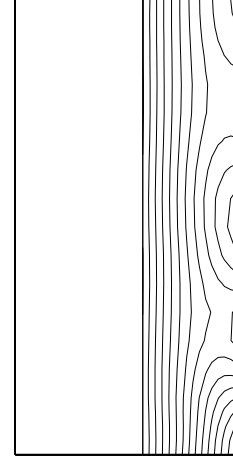
(2a)

$t=0.25, s=0.472, \theta_{\max}=0.752$



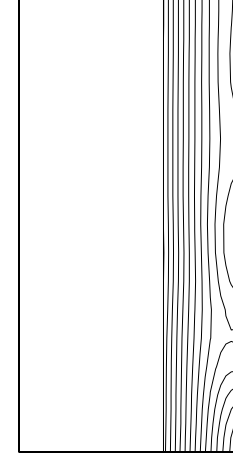
(3a)

$t=0.35, s=0.559, \theta_{\max}=0.230$



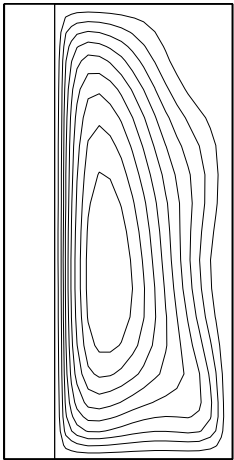
(4a)

$t=0.45, s=0.635, \theta_{\max}=0.047$



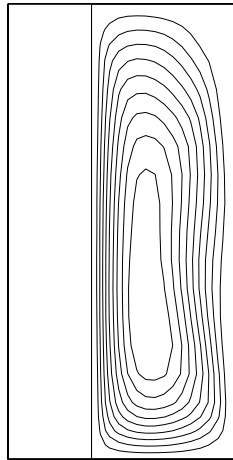
(5a)

$t=0.05, s=0.221, \psi_{\min}=-0.208$



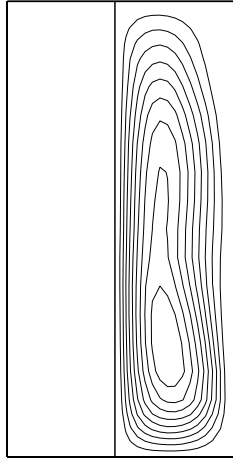
(1b)

$t=0.15, s=0.365, \psi_{\min}=-0.622$



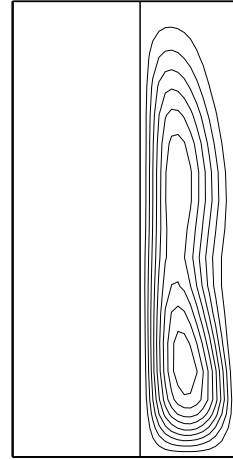
(2b)

$t=0.25, s=0.472, \psi_{\min}=-0.693$



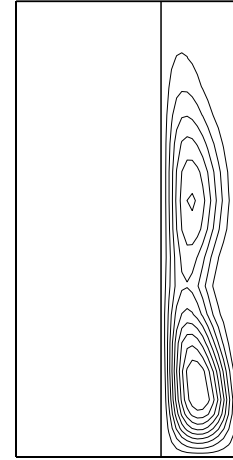
(3b)

$t=0.35, s=0.559, \psi_{\min}=-0.512$



(4b)

$t=0.45, s=0.635, \psi_{\min}=-0.284$



(5b)

**Figure 8: Temporal temperature and flow fields**